Original Research

CARDIAC RESEARCH

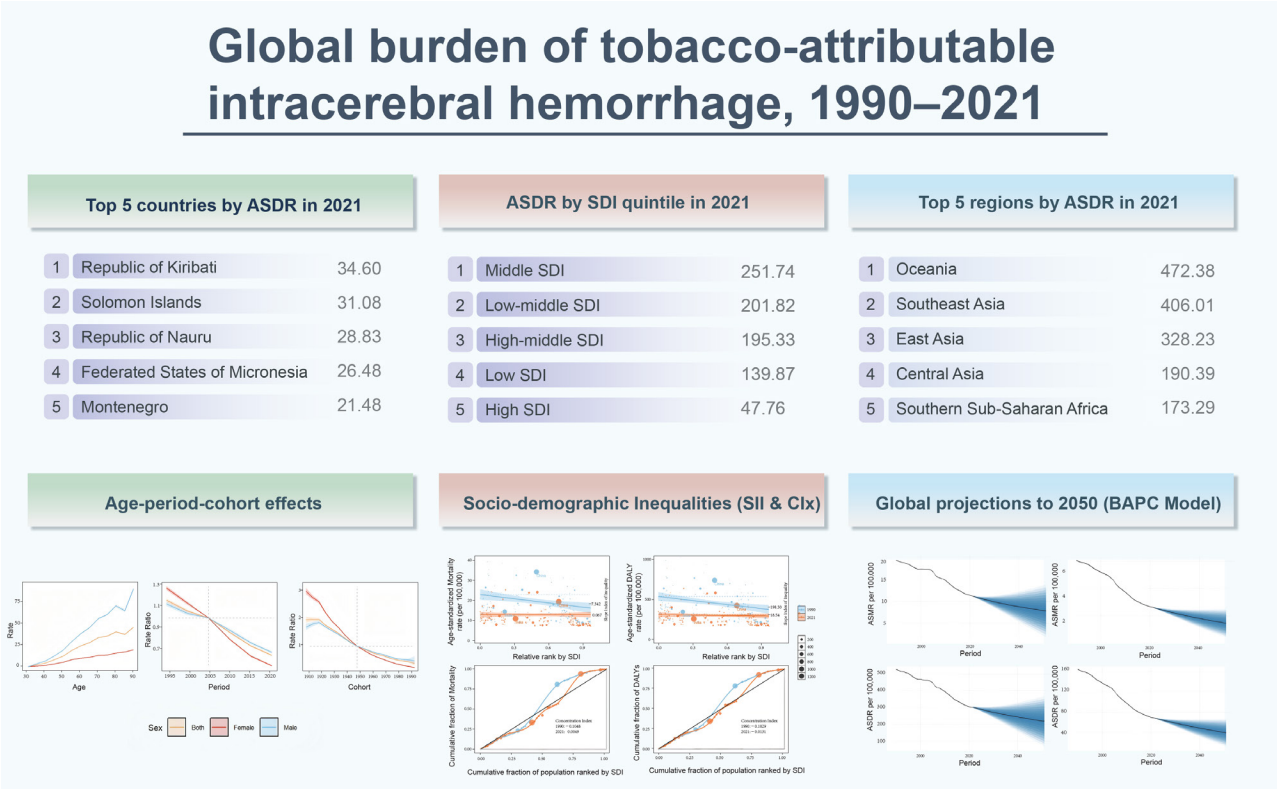
OPEN

Trends and sex-specific differences in tobacco-attributable intracerebral hemorrhage burden, 1990–2021

Age-period-cohort analyses and cross-country inequality based on the Global Burden of Disease Study 2021

Weizi Yang, MS[a,b,c], Xue Xia, PhD[a,b,c], Yunyi Hao, MS[a,b,c], Jinqing Zhao, MS[a,b,c], Xingquan Zhao, PhD[b,d,*], Anxin Wang, PhD[a,b,c,*]

Graphical abstract



WY and XX contributed to this article equally.

Supplemental Digital Content is available for this article.

[a] Department of Epidemiology, Beijing Neurosurgical Institute, Beijing Tiantan Hospital, Capital Medical University, Beijing, China, [b] China National Clinical Research Center for Neurological Diseases, Beijing Tiantan Hospital, Capital Medical University, Beijing, China, [c] Department of Clinical Epidemiology and Clinical Trial, Capital Medical University, Beijing, China, [d] Department of Neurology, Beijing Tiantan Hospital, Capital Medical University, Beijing, China.

* Correspondence: Xingquan Zhao, Department of Neurology, Beijing Tiantan Hospital, Capital Medical University, No.119 South 4th Ring West Road, Fengtai District, Beijing 100070, China (e-mail: zxq@vip.163.com); Anxin Wang, Department of Epidemiology, Beijing Neurosurgical Institute, Beijing Tiantan Hospital, Capital Medical University, No.119 South 4th Ring West Road, Fengtai District, Beijing 100070, China (e-mail: wanganxin@bjtth.org).

© The Author(s) 2026. Published by Wolters Kluwer Health, LLC. on behalf of Higher Education Press. This is an open access article distributed under the Creative Commons Attribution License 4.0 (CCBY), which permits unrestricted use, distribution, and reproduction in any medium, provided the original work is properly cited.

Cardiac Research (2026) 2:2

Received: 05 November 2025 / Received in final form: 14 April 2026 / Accepted: 21 May 2026

http://dx.doi.org/10.1097/re9.0000000000000020

Abstract

Background: This study evaluated the global burden of tobacco-attributable intracerebral hemorrhage (ICH) from 1990 to 2021, focusing on temporal trends, geographical disparities, and socio-demographic inequalities.

Methods: We calculated the estimated annual percentage change (EAPC) of age-standardized mortality rate (ASMR) and disability-adjusted life year rate (ASDR) to assess the changing trend. An age-period-cohort (APC) model was used to assess the effects of age, period, and cohort on the burden of ICH attributable to tobacco use, and the future trends till 2050 were further projected with a Bayesian age-period-cohort (BAPC) model. Cross-country inequalities were evaluated with the slope inequality index (SII) and the concentration index (CIx).

Results: In 2021, the ASMR and ASDR of tobacco-attributable ICH were 6.56/100,000 and 179.20/100,000. From 1990 to 2021, the EAPCs were –2.08 and –2.15, respectively. The highest burden was observed in middle sociodemographic index (SDI) countries, males, and Oceania. The EAPC analysis showed the fastest decline in high-SDI countries (ASMR: –3.57). The burden decreased more for females than for males. The age effects on global mortality and disability-adjusted life years attributed to tobacco increased with age, while period and cohort effects showed a continuous downward trend. Cross-country inequalities decreased significantly, although middle SDI countries remained heavily impacted.

Conclusion: Despite global progress in reducing the tobacco-related ICH burden, males and middle SDI countries remain disproportionately affected. Strengthening tobacco control policies and health education for high-risk populations is essential for further reductions and health equity.

Keywords: age-period-cohort analysis, Bayesian age-period-cohort model, disease burden, intracerebral hemorrhage

Abbreviations

APC	age-period-cohort
ASDR	age-standardized disability-adjusted life year rate
ASMR	age-standardized mortality rate
ASR, age	standardised rates
BAPC	bayesian age-period-cohort
CI	confidence interval
CIx	concentration index
CODEm	cause of death ensemble model
DALYs	disability-adjusted life years
EAPC	estimated annual percentage change
EDU15+	mean education for those aged 15 years and older
GAM	generalized additive models
GBD	global burden of disease
GLMs	generalized linear models
ICH	intracerebral hemorrhage
IHME	Institute for Health Metrics and Evaluation
INLA	integrated nested laplace approximations
LDI	lag distributed income per capita
MR-BRT	mixed-effects regression, bayesian, regularized, trimmed model
PAF	population attributable fraction
ROS	reactive oxygen species
RR	relative risks
SDI	socio-demographic index
SII	slope inequality index
TFU25	total fertility rate under 25 years
UI	uncertainty intervals
WHO	World Health Organization

Highlights

- Global tobacco-attributable intracerebral hemorrhage (ICH) burden declined significantly from 1990 to 2021.
- Males and middle sociodemographic index countries bear the highest burden of tobacco-related ICH.
- Age effects on ICH mortality and disability-adjusted life years increased sharply with advancing age.
- Period and cohort effects showed consistent downward trends, especially in females.
- Cross-country health inequalities in ICH burden narrowed substantially by 2021.
- Targeted tobacco control in high-risk populations and regions remains critical.

1. Introduction

In 2021, intracerebral hemorrhage (ICH) was a major cause of death and disability-adjusted life years (DALYs) worldwide.[1] Despite accounting for only 28.8% of all incident strokes, ICH constituted the largest proportion of all DALYs due to stroke (49.6%).[2] Research shows that only half of patients survive for 1 year after ICH, and those survivors often experience long-term sequelae that significantly impact their quality of life.[3] Globally, ICH was the sixth-leading cause of global DALYs at 79.5 million, causing 3.31 million deaths. Consequently, ICH is a severe condition in which studies have demonstrated that ICH has resulted in a considerable social and economic burden and has emerged as a prominent public health concern.[4]

Tobacco smoking is a significant contributor to preventable morbidity and mortality on a global scale.[5] There is substantial evidence that tobacco use is a major risk

factor for the development of cerebral hemorrhage.[6–8] For example, the existing literature demonstrates that cigarette smoking not only increases the risk of ICH but also increases hematoma growth, results in worse outcomes, and increases the risk of death from ICH.[9,10] Furthermore, the global burden of disease (GBD) 2021 risk factors collaborators identified tobacco as one of the top 3 risk factors for ICH. This may be due to the temporary elevation of blood pressure triggered by smoking, as well as the disruption of the integrity of the blood–brain barrier by tobacco use, increased production of reactive oxygen species, and activation of proinflammatory pathways. Together, these factors increase the risk of ICH and its possible adverse consequences.[11–14]

Although studies have examined the association between smoking and ICH, a significant gap remains in the comprehensive, dynamic, and forward-looking assessment of the smoking-attributable ICH disease burden. While previous GBD-based studies have updated burden estimates, most are limited to describing trends in age-standardized rates (ASRs). They often lack decomposition of the underlying age, period, and cohort effects driving these trends and fail to fully utilize model parameters for long-term forecasting. Furthermore, systematic assessments of health inequalities across regions with different socioeconomic development levels are notably insufficient. Therefore, this study aims to address the following critical knowledge gaps by integrating the full dataset from GBD 2021[1,15] and employing the age-period-cohort (APC) model and Bayesian APC (BAPC) forecasting framework: First, to quantify the long-term trends and their driving factors (age, period, and cohort effects) of smoking-attributable ICH mortality and DALYs burden from 1990 to 2021 at the global, regional, and sociodemographic index (SDI) levels. Second, to project the future disease burden from 2022 to 2050 based on historical trends. Third, to comprehensively evaluate the distribution disparities and health inequalities of the attributable burden across sexes and SDI regions. By providing this multidimensional, dynamic, and prospective analysis, this study aims to offer more precise empirical evidence for formulating targeted tobacco control policies and ICH prevention strategies.

2. Methods

2.1. Overview

The present study is based on the framework of the GBD 2021 that provides systematic estimates of health loss for 369 diseases and injuries and 88 risk factors across 204 countries and 811 subnational locations, using standardized and comparable methodology.[1,15] The core analytical tools include the cause of death ensemble model for mortality estimation and Bayesian meta-regression disease modeling software (DisMod-MR 2.1, Institute for Health Metrics and Evaluation, Washington) for nonfatal outcomes (incidence, prevalence, and disability weights). These methods ensure global comparability and allow for the decomposition of the burden into fatal and nonfatal components. The GBD database has been instrumental in facilitating numerous epidemiological studies on the burden of various diseases, thereby providing an effective reference point for the formulation of adaptive public health decisions and the allocation of health resources in different countries around the world.[16,17] This study directly extracted the relevant data on the burden of hemorrhagic stroke attributable to tobacco use from the GBD 2021 output. Within a unified methodological framework, this study analyzed the ASRs of hemorrhagic stroke burden attributable to tobacco use from 1990 to 2021, with stratification by sex, age, geographic region, and country. The analysis systematically elucidates the contribution of tobacco use to the disease burden of hemorrhagic stroke.

2.2. Case definitions and attribution

In the GBD 2021 classification, ICH is defined as a rupture of a blood vessel resulting in nontraumatic ICH (ICD-10 code: I61). The definition of ICH meets the World Health Organization (WHO) criteria for the rapid onset of clinical symptoms of cerebral dysfunction (usually focal) lasting more than 24 h or resulting in death.[18] In the GBD 2021 study, tobacco use was defined as encompassing the use of tobacco in any form, including smoking, chewing, and exposure to secondhand smoke.[19] All estimates of the tobacco-attributable ICH burden used in this study (including ASRs and uncertainty intervals [UIs]) were directly sourced from the final GBD 2021 output. The attributable burden of ICH due to tobacco use was quantified by the Institute for Health Metrics and Evaluation (IHME), with the core method centered on multiplying the population-attributable fraction by relevant disease outcome metrics. Detailed procedures are provided in the supplementary materials.

2.3. Statistical analysis

2.3.1. Trend analysis. In order to quantify the epidemic trends of ICH attributed to tobacco, the ASRs and their estimated annual percentage change (EAPC) were calculated. ASR is derived from a weighted average of rates at specific ages. To illustrate the long-term trajectory of the age-standardized mortality rate (ASMR) and disability-adjusted life year rate (ASDR) from 1990 to 2021, we calculated the EAPC. The EAPC was derived from a regression model that was constructed by fitting the natural logarithm to the calendar year ($Y = \alpha + \beta X + \varepsilon$), where Y represents the natural logarithm of the rate, X denotes the calendar year, and ε represents the error term. EAPC with its 95 % confidence interval (CI) was calculated on a log scale from the model $100 \times (\exp(\beta) - 1)$.[20]

2.3.2. Descriptive subgroup and inequality analysis. Subgroup analyses were performed by stratifying the

burden estimates (ASMR and ASDR) according to sex, geographical region, and SDI levels. The study collated ASR of ICH attributable to tobacco between 1990 and 2021, disaggregated by sex, age, region, and country, along with the estimates and their 95% UIs for mortality and DALYs. The SDI was employed as a composite measure of the comprehensive development status of countries and regions. Proposed by the IHME, the SDI combines three components: lag-distributed income per capita, mean education for those aged 15 and older, and the total fertility rate under 25. For analytical purposes, the 204 countries and territories were categorized into five groups (low, low-middle, middle, high-middle, and high) based on the quintiles of the country-level SDI estimates for the year 2021.

To assess global disparities in ASDR and ASMR, we employed the slope inequality index (SII) and concentration index (CIx) as standardized indicators.[21,22] The SII is a measure that quantifies the absolute degree of inequality in health indicators between the most advantaged and least advantaged groups of the population.[23] The CIx represents a quantitative measure of relative inequality, indicating the extent to which a given health indicator is concentrated among the disadvantaged or advantaged. A positive CIx indicates concentration in higher SDI countries, while a negative CIx indicates concentration in lower SDI countries.[23]

2.3.3. APC model analysis. This study employs an APC model framework to analyze trends over time in mortality and DALY rates for smoking-attributable ICH and to decompose the underlying age, period, and birth cohorts[24] effects. The APC model effectively distinguishes and quantifies 3 fundamental and often intertwined temporal dimensions within long-term trends: the age effect, which reflects changes in disease risk associated with physiological aging; the period effect, capturing external factors that influence all age groups at specific historical points in time; and the cohort effect, revealing the unique risk profile of generations sharing a common birth year and thus similar early-life exposures and sociobehavioral patterns.[25] This distinction is crucial for understanding the drivers of disease burden and for formulating long-term public health strategies.

Regarding data preparation, in accordance with the study design, mortality and DALY data were organized into 15 consecutive 5-year age groups (from 25–29 to 85 years and above) and six 5-year periods (1992–1996 to 2017–2021). Corresponding birth cohorts were derived for analysis. The APC model estimates provide interpretation for the following key parameters: the drift, expressed as an annual percentage change, represents the overall average annual trend in the ASMR or ASDR, with its sign indicating an overall increase or decrease in disease burden. The local drift quantifies the heterogeneity of this trend across different age groups, useful for identifying differences in the pace of disease burden change across the age distribution. The age effect is illustrated by the longitudinal age curve, depicting the intrinsic pattern of how disease risk changes with age after controlling for period and cohort influences. The period and cohort effects are presented as period relative risks (RRs) and cohort RR.[26] This study utilized a web-based APC model tool for parameter estimation. The statistical significance of trends was assessed using the Wald χ^2 test, with a p-value < 0.05 considered statistically significant.[24]

2.3.4. Predictive analysis. We employed a BAPC model using integrated nested Laplace approximations (INLA) to project disease burden from 2022 to 2050.[27,28] The model assumes that case counts follow a Poisson distribution and incorporates random effects for age, period, and cohort, each smoothed via second-order random walk priors; all priors were set to their default specifications within the INLA framework. An independent and identically distributed random effect is also included to adjust for overdispersion. The BAPC model was selected primarily due to its relatively high prediction coverage and good calibration performance even with short observation periods, making it particularly suitable for trend extrapolation when long-term surveillance data is limited. Compared with traditional generalized linear models, generalized additive models, or the mixed-effects regression, bayesian, regularized, trimmed model (MR-BRT) commonly used in the GBD study, the BAPC model can simultaneously capture the structural influences of age, period, and cohort while providing a complete posterior predictive distribution to quantify uncertainty. The model relies on the following key assumptions: historical age, period, and cohort effects remain smooth and continue throughout the projection period; demographic changes are incorporated through age-specific population data; and no sudden impacts from major future policies or technological breakthroughs on incidence are considered. As the projection horizon extends, prediction uncertainty gradually increases, manifested by widening posterior standard deviations and broader credible intervals.[29] In this study, we utilized the BAPC package and the INLA package in the *R* programming language (*R*) to conduct BAPC model calculations and analyses.[30,31]

All statistical analyses except APC analyses were performed in R version 4.3.3 (R Core Team under the auspices of the R Foundation). The ASDR was reported per 100,000 population along with a 95% UI. SII, CIx, and EAPC were all presented with their respective 95% CI. A 2-sided p-value < 0.05 indicated statistical significance.

3. Result

3.1. Epidemic trends of ICH attributable to tobacco from 1990 to 2021

Table 1 and Table S1, Supplemental Digital Content, https://links.lww.com/CARES/A16, present the changes in ASMR and ASDR attributed to tobacco globally for ICH between the years 1990 and 2021. The rates

Table 1

ASMR, ASDR, and EAPC of ICH attributed to tobacco in global countries with different SDI levels and regions of the world from 1990 to 2021.

	ASMR (per 100,000)			ASDR (per 100,000)		
	In 1990 (95% UI)	In 2021 (95% UI)	EAPC (95% CI)	In 1990 (95% UI)	In 2021(95% UI)	EAPC (95% CI)
Global	12.04 (9.72, 14.44)	6.56 (5.29, 8.01)	−2.08 (−2.22, −1.93)	337.56 (281.82, 398.47)	179.20 (147.04, 214.88)	−2.15 (−2.28, −2.01)
High SDI	4.36 (3.73, 5.10)	1.54 (1.27, 1.83)	−3.57 (−3.66, −3.48)	130.77 (113.40, 149.67)	47.76 (39.68, 56.10)	−3.41 (−3.49, −3.34)
High-middle SDI	14.41 (11.75, 17.29)	7.27 (5.78, 9.19)	−2.48 (−2.79, −2.17)	398.72 (332.59, 471.13)	195.33 (158.10, 238.94)	−2.57 (−2.86, −2.27)
Middle SDI	19.15 (15.20, 23.85)	9.93 (7.75, 12.41)	−2.13 (−2.28, −1.98)	498.24 (402.46, 609.46)	251.74 (201.44, 306.21)	−2.19 (−2.31, −2.06)
Low-middle SDI	12.46 (9.85, 15.10)	7.22 (5.73, 8.73)	−1.83 (−1.88, −1.78)	351.06 (281.96, 420.77)	201.82 (162.19, 243.17)	−1.83 (−1.88, −1.79)
Low SDI	8.94 (6.89, 11.26)	4.94 (3.78, 6.25)	−2.08 (−2.17, −1.99)	253.81 (197.99, 318.44)	139.87 (108.15, 175.46)	−2.13 (−2.22, −2.03)
Andean Latin America	3.39 (2.66, 4.19)	1.16 (0.86, 1.55)	−3.84 (−4.10, −3.58)	102.76 (80.61, 126.41)	35.37 (26.29, 46.85)	−3.80 (−4.06, −3.54)
Australasia	1.97 (1.60, 2.38)	0.53 (0.42, 0.65)	−4.24 (−4.36, −4.11)	55.12 (45.92, 65.13)	15.26 (12.50, 18.52)	−4.15 (−4.31, −3.99)
Caribbean	6.69 (5.55, 8.05)	3.37 (2.64, 4.20)	−2.39 (−2.54, −2.25)	201.74 (168.65, 239.97)	101.26 (80.18, 124.87)	−2.38 (−2.54, −2.22)
Central Asia	10.67 (8.79, 12.77)	6.77 (5.37, 8.20)	−1.72 (−2.24, −1.20)	318.01 (264.29, 376.94)	190.39 (153.89, 228.33)	−2.01 (−2.52, −1.50)
Central Europe	10.85 (9.14, 12.74)	3.43 (2.80, 4.09)	−4.40 (−4.69, −4.12)	322.24 (277.17, 371.10)	99.91 (82.50, 116.97)	−4.47 (−4.76, −4.19)
Central Latin America	3.54 (2.87, 4.23)	1.21 (0.94, 1.53)	−4.08 (−4.29, −3.87)	101.08 (83.09, 118.78)	35.86 (27.98, 44.70)	−3.96 (−4.19, −3.73)
Central Sub-Saharan Africa	6.95 (5.04, 9.34)	4.37 (3.05, 5.99)	−1.60 (−1.73, −1.47)	202.38 (147.37, 269.06)	127.56 (90.23, 175.61)	−1.59 (−1.72, −1.45)
East Asia	29.41 (22.78, 36.72)	13.59 (10.31, 17.30)	−2.50 (−2.74, −2.25)	711.67 (570.22, 890.45)	328.23 (252.59, 412.71)	−2.49 (−2.70, −2.28)
Eastern Europe	6.15 (5.19, 7.14)	4.41 (3.65, 5.15)	−1.96 (−2.68, −1.23)	197.12 (168.95, 225.35)	152.33 (127.07, 176.19)	−1.73 (−2.46, −0.99)
Eastern Sub-Saharan Africa	11.06 (8.68, 13.98)	5.15 (4.02, 6.59)	−2.72 (−2.85, −2.60)	310.39 (243.69, 388.54)	146.93 (114.31, 187.22)	−2.67 (−2.79, −2.55)
High-income Asia Pacific	6.65 (5.53, 7.77)	1.52 (1.26, 1.82)	−4.93 (−5.08, −4.79)	198.37 (169.36, 226.45)	50.07 (42.14, 58.43)	−4.65 (−4.78, −4.50)
High-income North America	2.20 (1.86, 2.57)	1.26 (1.05, 1.53)	−2.00 (−2.15, −1.85)	68.59 (58.88, 79.72)	38.89 (32.12, 46.19)	−2.00 (−2.11, −1.88)
North Africa and Middle East	9.18 (7.19, 11.18)	3.60 (2.81, 4.54)	−3.30 (−3.45, −3.16)	258.78 (205.70, 310.68)	102.23 (80.16, 127.20)	−3.28 (−3.41, −3.15)
Oceania	22.05 (15.59, 29.05)	16.30 (11.69, 21.42)	−1.08 (−1.13, −1.02)	636.48 (453.35, 828.87)	472.38 (342.46, 624.47)	−1.06 (−1.12, −1.01)
South Asia	9.77 (7.59, 12.15)	5.31 (4.01, 6.65)	−2.02 (−2.08, −1.96)	270.17 (211.62, 333.11)	145.33 (111.46, 180.18)	−2.04 (−2.09, −1.98)
Southeast Asia	21.77 (17.41, 26.31)	14.02 (11.14, 17.10)	−1.46 (−1.57, −1.36)	612.04 (504.33, 731.59)	406.01 (325.92, 490.26)	−1.32 (−1.41, −1.24)
Southern Latin America	8.20 (6.85, 9.62)	2.24 (1.83, 2.70)	−4.27 (−4.42, −4.11)	270.80 (229.47, 314.60)	73.02 (60.35, 85.94)	−4.36 (−4.52, −4.19)
Southern Sub-Saharan Africa	9.12 (7.18, 11.23)	5.81 (4.61, 7.08)	−1.44 (−1.81, −1.07)	283.45 (228.41, 343.13)	173.29 (139.34, 209.04)	−1.55 (−1.90, −1.21)
Tropical Latin America	12.15 (10.26, 14.14)	2.46 (2.02, 2.99)	−5.46 (−5.58, −5.33)	381.55 (326.55, 435.54)	73.89 (60.64, 89.48)	−5.66 (−5.79, −5.52)
Western Europe	3.48 (2.93, 4.06)	0.96 (0.79, 1.17)	−4.28 (−4.38, −4.19)	99.48 (85.42, 114.75)	27.07 (22.83, 32.04)	−4.36 (−4.44, −4.27)
Western Sub-Saharan Africa	5.21 (3.82, 6.87)	2.94 (2.13, 3.77)	−2.02 (−2.18, −1.87)	155.92 (113.99, 202.34)	89.16 (64.61, 114.11)	−1.99 (−2.16, −1.83)

ASDR = age-standardized DALY rate; ASMR = age-standardized mortality rate; CI = confidence interval; DALYs = disability-adjusted life years; EAPC = estimated annual percentage change; ICH = intracerebral hemorrhage; SDI = sociodemographic index; UI = uncertainty intervals.

demonstrated a notable decline from 12.04/100,000 and 337.56/100,000 in 1990 to 6.56/100,000 and 179.20/100,000 in 2021, respectively. The EAPCs were −2.08 (95% CI: −2.22 to −1.93) and −2.15 (95% CI: −2.28 to −2.01), respectively. In 2021, the top 3 geographical regions with the highest ASMR and ASDR were Oceania, Southeast Asia, and East Asia. As illustrated in Table 1, between 1990 and 2021, Tropical Latin America saw the largest declines in ASMR and ASDR, with EAPCs of −5.46 (95% CI: −5.58 to −5.33) and −5.66 (95% CI: −5.79 to −5.52), respectively.

During 1990 to 2021, the ASMR and ASDR of countries with middle SDI remained the highest among all the SDI regions, ranging from 19.15/100,000 to 9.93/100,000 and from 498.24/100,000 to 251.74/100,000, respectively. In contrast, the high-SDI country displayed the lowest ASMR and ASDR. All SDI-level countries displayed a decreasing trend in ASMR and ASDR, with EAPC values below zero. The EAPC for ASMR and ASDR was lowest in high-SDI countries and highest in low-middle SDI countries.

Table S2, Supplemental Digital Content, https://links.lww.com/CARES/A16, and Figure S1, Supplemental Digital Content, https://links.lww.com/CARES/A16, illustrate the gender distribution of the burden of tobacco-attributable ICH from 1990 to 2021. On a global scale, there was a significant decrease in the number of deaths and DALYs attributable to ICH for both men and women. However, the decline was more pronounced for women. It is intriguing to observe that gender differences emerge in countries with varying levels of SDI. In the middle SDI country, the EAPC for ASMR and ASDR was −1.66 (95% CI: −1.82 to −1.49) and −1.76 (95% CI: −1.90 to −1.62) in males, respectively, while it was −3.46 (95% CI: −3.63 to −3.29) and −3.53 (95% CI: −3.67 to −3.39) in females, which is more than double the rate observed in males. Conversely, the disparity between male and female EAPC was less pronounced in low and high-SDI countries.

3.2. Cross-country inequality analysis of the ICH burden attributable to tobacco

In 1990, considerable absolute and relative SDI-related inequalities were observed in the ICH burden attributable to tobacco. However, by 2021, these inequalities had diminished significantly (Fig. 1). In 1990, a higher prevalence was observed to disproportionately concentrate in countries with a lower SDI. The SII of mortality in 1990 was −7.342, indicating that the countries with the highest SDI in 1990 had 7.342 fewer deaths (per 100,000 population) than the countries with the lowest SDI, and this indicator was reduced to 0.067 in 2021. Concomitantly, the CIx exhibited a downward trajectory from 1990 to 2021. The CIx of mortality exhibited a notable decline from −0.1048 in 1990 to 0.0049 in 2021. The CIx of DALYs was −0.1029 in 1990 and subsequently decreased to −0.0131.

3.3. APC analysis of the ICH burden attributable to tobacco use

The APC analysis revealed distinct patterns in tobacco-attributable ICH burden globally (Fig. 2 and Tables S3–S6, Supplemental Digital Content, https://links.lww.com/CARES/A16).

Age effects demonstrated a sharp, continuous increase in mortality rates with advancing age for both sexes. Male mortality rose from 0.43 (95% CI: 0.38–0.49) in ages 25–29 years to 92.13 (95% CI: 89.61–94.72) in ages ≥ 85 years, while female mortality increased from 0.74 (95% CI: 0.69–0.78) to 20.38 (95% CI: 19.97–20.79) over the same age range. The age effect on DALYs peaked earlier, at 55–59 years for females (368.64, 95% CI: 363.68–373.67) and at 65–69 years for males (1,412.86, 95% CI: 1,387.11–1,439.08).

Period effects showed a consistent global decline in both mortality and DALYs from 1992 to 2021, with a more pronounced reduction in females. Compared with the 2002–2006 reference period, the RR of mortality for females fell from 1.27 (95% CI: 1.25–1.28) in 1992–1996 to 0.58 (95% CI: 0.57–0.59) in 2017–2021. A similar declining trend was observed for males. The RR dropped from 1.13 (95% CI: 1.11–1.15) in 1992–1996 to 0.70 (95% CI: 0.68–0.71) in 2017–2021.

Birth cohort effects also indicated a sustained downward trend in RR for successive cohorts, with a steeper decline among females. Relative to the reference cohort, the mortality RR for females born in 1905–1909 was 3.03 (95% CI: 2.92–3.15), declining to 0.22 (95% CI: 0.19–0.25) for those born in 1990–1994. For males, the RR decreased from 1.71 (95% CI: 1.60–1.83) in the 1905–1909 cohort to 0.47 (95% CI: 0.35–0.64) in the 1990–1994 cohort.

3.4. Projections of the global trends of ICH attributable to tobacco until 2050

As depicted in Figure 3 and Table S7, Supplemental Digital Content, https://links.lww.com/CARES/A16, projections indicate that both ASMR and ASDR will continue their downward trajectory over the next 3 decades. Males are expected to maintain higher rates than females throughout this period. For females, the ASMR is forecasted to show a decline from 2.62/100,000 in 2021 to an estimated 1.51/100,000 by 2050 (95% CI: 0.52–2.50). In parallel, the ASDR for females is anticipated to drop from 68.58/100,000 in 2021 to 40.27/100,000 by 2050 (95% CI: 14.58–65.96). By 2050, the male ASMR is projected to decline from 11.11/100,000 in 2021 to 7.91/100,000 (95% CI: 2.26–13.56), while the male ASDR is expected to decrease from 298.56/100,000 in 2021 to 219.56/100,000 (95% CI: 77.46–361.66).

4. Discussion

The burden of ICH attributable to tobacco exhibited significant spatial variation, with a 69-fold and 82-fold

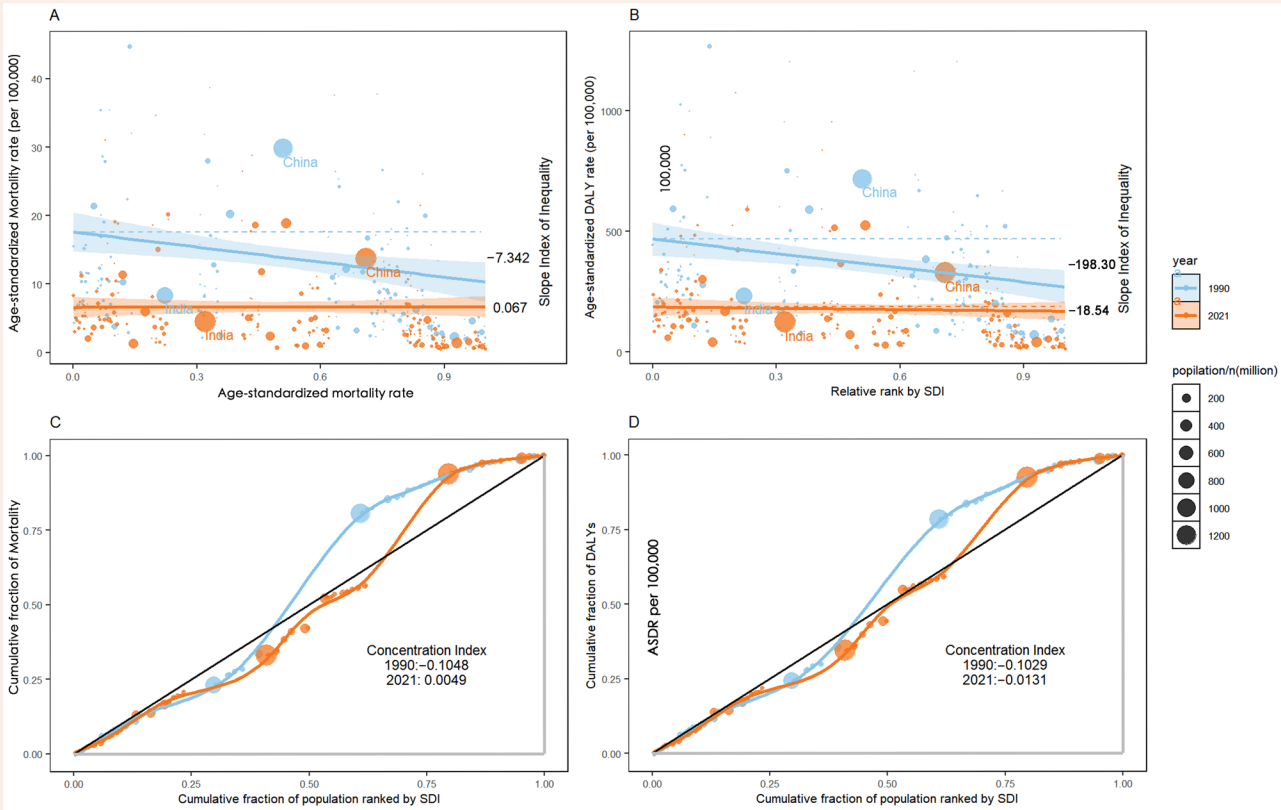


Figure 1. Slope indexes and concentration indexes for ICH mortality and DALYs attributable to tobacco from 1990 to 2021 worldwide. (A) Health inequality regression curve for ICH mortality. (B) Health inequality regression curve for ICH DALYs. (C) Concentration curves for ICH mortality. (D) Concentration curves for ICH DALYs. DALYs = disability-adjusted life years; ICH = intracerebral hemorrhage.

difference in ASMR and ASDR, respectively, between the top and bottom-ranked countries. Furthermore, there are significant differences between countries with disparate SDI levels. Nations with a moderate SDI exhibited the highest ASR in comparison to other countries. Conversely, countries with high and low SDI exhibited the lowest ASR. This variation may be attributed to a complex interplay of multiple factors. Firstly, there is a substantial variation in tobacco exposure levels across different SDI levels. The study indicated China, India, and Indonesia as the countries with the highest number of smokers, collectively accounting for nearly half of the global smoking population. China is classified as a high-middle SDI country, while India and Indonesia are designated as middle SDI countries. This suggests that the proportion of smokers is more concentrated in countries with a middle or high-middle SDI.[32] Moreover, in comparison with high-SDI countries, middle-SDI countries frequently encounter challenges such as unequal resource distribution, an underdeveloped healthcare system, and inadequate health education, which result in deficiencies in the prevention, early recognition, and treatment of ICH.[33] The higher prevalence of ICH in middle SDI countries can be attributed to a number of factors, including low levels of education, weak health awareness, difficulties in accessing healthcare resources, and inadequate primary and secondary prevention measures.[34] With regard to the EAPC of ASR in different SDI countries, it is evident that the decline trend is most rapid in countries with high-SDI levels and least rapid in low-middle SDI and low SDI countries. This is attributable to the fact that high-SDI countries are able to benefit from a robust economic foundation and advanced public health policies, which enable them to more effectively control the risk factors for ICH and achieve early diagnosis and effective treatment of the disease through a well-developed healthcare system.[35] The extensive health education and abundant medical resources in these countries provide strong support for the comprehensive management of ICH. This concentration of burden highlights a critical public health imperative. Resource allocation and global health initiatives must be strategically directed towards middle SDI countries. The substantial population-attributable risk in these regions indicates that interventions successfully reducing tobacco use and improving hypertension control would yield disproportionately large benefits in reducing the overall global ICH burden.

The burden of ICH attributable to tobacco was found to be higher in males than in females. However, females have exhibited a more pronounced decrease in the ASR of ICH burden. It has been suggested that, compared with nonsmokers, the excess risk of stroke is at least as

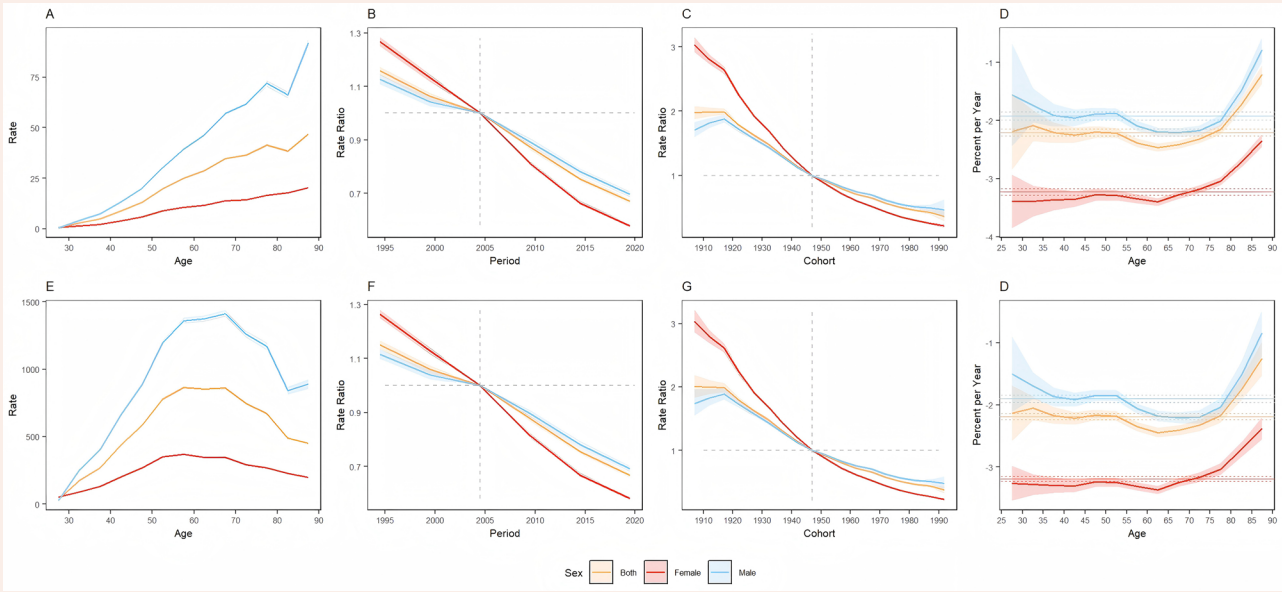


Figure 2. Parameter estimates of age, period, and cohort effects on ICH mortality and DALYs attributable to tobacco from 1990 to 2021. (A) The longitudinal rates of ICH mortality. (B) The relative risk of ICH mortality. (C) The relative risk of ICH mortality. (D) The local drifts of ICH mortality. (E) The longitudinal rates of ICH DALYs. (F) The relative risk of ICH DALYs. (G) The relative risk of ICH DALYs. (H) The local drifts of ICH DALYs. DALYs = disability-adjusted life years; ICH = intracerebral hemorrhage.

great among women who smoke as it is among men who smoke.[36] It can, therefore, be concluded that the gender differences in ICH attributed to tobacco are mainly due to the differences in smoking rates between males and females. A review of the literature reveals that in 2019, the smoking rate among males was 5 times that of females.[37] This discrepancy has direct implications for tailored public health messaging and clinical outreach. While male-focused campaigns remain crucial given their higher prevalence, the elevated RR in female smokers necessitates that cessation programs and health warnings actively address and engage women, ensuring they are not overlooked in tobacco control efforts.

The analysis revealed that age is a significant risk factor, as evidenced by the observed increase in the longitudinal rates of ICH mortality with age. In all age groups, males consistently exhibited a higher mortality rate than females. This disparity may be attributed to the fact that the pathogenesis of ICH is influenced by a multitude of factors that are intricately linked to the aging process. These include alterations in vascular structure and function, an augmented inflammatory response, and a compromised immune system.[38] From a public health perspective, the age-effect curve, which peaks in the 55 to 60 age group, underscores a critical window for intervention. This mandates targeted risk assessment and proactive patient education for individuals approaching and within this high-risk bracket. Healthcare providers should integrate intensified cardiovascular risk screening, including blood pressure monitoring and counseling on lifestyle modifications, into routine care for this demographic.

The period effect indicated a persistent downward trend in global mortality and DALYs. The ongoing decline may be largely attributed to the heightened public awareness of the detrimental effects of smoking,[39] in conjunction with the implementation of a series of comprehensive tobacco control policies, which have led to a reduction in smoking rates and subsequently an impact on the incidence of ICH.[40] For example, the WHO proposed the Framework Convention on Tobacco Control and MPOWER measures.[41] A substantial number of countries have enacted national legislation aimed at reducing the prevalence of tobacco smoking.[42] Moreover, developments in medical technology, including more efficacious treatments and management strategies for ICH, have also played a pivotal role in shaping the prognosis of ICH across various time periods.[43] However, it is crucial to acknowledge that the rate of progress has slowed in a considerable number of countries, including those that had previously witnessed a notable decline in incidence, particularly over the past decade. Consequently, it is paramount that we reinforce the implementation of antismoking legislation and public health initiatives to sustain the momentum of this progress.

This study elucidates the long-term trends and cross-national disparities in the burden of tobacco-induced ICH, providing an evidence-based foundation for formulating public health strategies. The findings advocate for a multi-pronged strategic framework. Within healthcare delivery systems, implementing targeted risk assessments alongside tailored patient education for high-risk demographics, particularly males aged 55 and above, is warranted. Geostrategic priorities should focus

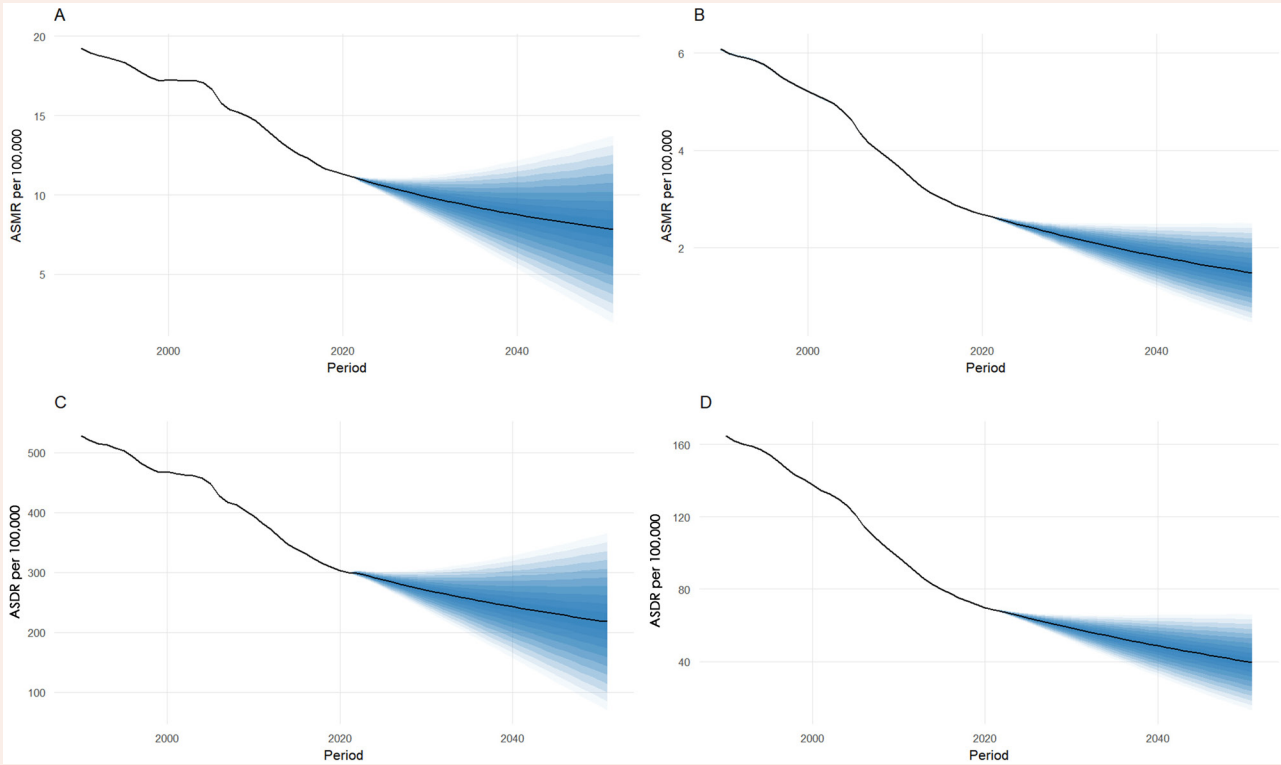


Figure 3. Projections of the global trends of ICH attributable to tobacco until 2050 based on the BAPC model. (A) ICH mortality attributable to tobacco in males. (B) ICH mortality attributable to tobacco in females. (C) ICH DALYs attributable to tobacco in males. (D) ICH DALYs attributable to tobacco in females. BAPC = Bayesian age-period-cohort; DALYs = disability-adjusted life years; ICH = intracerebral hemorrhage.

on middle SDI countries—such as high-burden regions in East Asia and Oceania—advancing beyond general tobacco control towards integrated interventions. These measures could combine enhanced hypertension screening and management protocols with intensive, culturally adapted smoking cessation programs, further reinforced by focused health education campaigns for key populations. Furthermore, addressing the recent stagnation in progress necessitates sustained policy innovation and investment. This includes strengthening the implementation of proven measures like the WHO MPOWER package while exploring complementary strategies such as digital cessation tools and fiscal policies. The systematic execution of this coordinated framework is anticipated to reduce smoking prevalence, safeguard vulnerable populations, and contribute to improved public health outcomes.

This study employs a comprehensive analytical framework integrating EAPC, APC analysis, BAPC projection, and inequality indices (SII/CIx). The BAPC model is particularly advantageous, as it surpasses traditional time-series models by explicitly modeling the age, period, and cohort effects essential for understanding ICH trends shaped by aging and generational smoking patterns. This "EAPC + APC + BAPC + SII/CIx" framework is also broadly applicable to the assessment of other tobacco-related diseases.

Our study also has certain limitations. First, the modeling methods and data quality relied upon for GBD estimation may vary across different periods and regions, which could introduce certain biases into the burden of disease estimates. Second, this study is based on the GBD 2021 dataset, while the updated GBD 2023 results have already been released. Future research could further validate the current findings by incorporating the latest data. Third, it should be explicitly noted that the APC results are derived from GBD modeled rates rather than raw registry data, and, therefore, may reflect the modeling assumptions and adjustments applied in the GBD estimation process. Fourth, this study employs APC analysis based on cross-sectional data rather than a longitudinal follow-up design. Therefore, caution should be exercised when extrapolating population-level trends to individual-level interpretations. Finally, long-term trend projections are primarily based on extrapolations from historical data and assume that existing social, economic, and public health conditions remain largely unchanged. Thus, the projection results reflect more of a plausible scenario based on current conditions.

5. Conclusion

Despite a notable reduction in the mortality rate associated with ICH due to tobacco use over the past 3 decades, the

overall burden of ICH remains considerable, particularly in regions with middle SDI levels. The analysis demonstrates that the decline in the burden of ICH attributable to tobacco has been more pronounced in females than in males, yet the death burden in males remains higher. Period and cohort effects indicate favorable trends, but the downward trend is slowing. Furthermore, inequality between countries has fallen. In the context of ongoing global health challenges, our results emphasize the need for heightened attention and targeted strategies to mitigate the impact of tobacco-related ICH and protect public health.

Acknowledgements

We appreciate the invaluable work by the GBD, Injuries, and risk factors study 2021. We also express gratitude to the IHME for making the GBD data available for this research.

Ethical statement

This study used publicly available, de-identified aggregated data from the Global Burden of Disease Study 2021 (GBD 2021) maintained by the Institute for Health Metrics and Evaluation (IHME). As no identifiable human subjects were involved, institutional review board approval and individual informed consent were not required.

Conflicts of interest

The authors have no conflicts of interest to disclose.

Funding source

This study was funded by Beijing Natural Science Foundation Haidian Original Innovation Joint Fund (L222123).

Data availability statement

Data used for the analyses are publicly available from the Institute of Health Metrics and Evaluation.

Author contributions

Conceptualization: Anxin Wang, Xingquan Zhao, Weizi Yang, Xue Xia. Data curation & Formal analysis: Weizi Yang, Xue Xia, Yunyi Hao, Jinqing Zhao. Writing – original draft: Weizi Yang, Xue Xia. Writing – review & editing: Xue Xia, Anxin Wang, Xingquan Zhao. All authors read and approved the final manuscript. All authors read and approved the final manuscript.

AI statement

During the preparation of this work, the author used AI tools for language and grammar polishing. After using the tool, the author reviewed and edited the content as needed and takes full responsibility for the content of the published article.

References

[1] Ferrari AJ, Santomauro DF, Aali A, et al. Global incidence, prevalence, years lived with disability (YLDs), disability-adjusted life-years (DALYs), and healthy life expectancy (HALE) for 371 diseases and injuries in 204 countries and territories and 811 subnational locations, 1990–2021: a systematic analysis for the global burden of disease study 2021. Lancet. 2024;403:2133–61.

[2] GBD 2021 Stroke Risk Factor Collaborators. Global, regional, and national burden of stroke and its risk factors, 1990-2021: a systematic analysis for the Global Burden of Disease Study 2021. Lancet Neurol. 2024;23:973–1003.

[3] Puy L, Parry-Jones AR, Sandset EC, Dowlatshahi D, Ziai W, Cordonnier C. Intracerebral haemorrhage. Nat Rev Dis Primers. 2023;9:14.

[4] Xu L, Wang Z, Wu W, Li M, Li Q. Global, regional, and national burden of intracerebral hemorrhage and its attributable risk factors from 1990 to 2021: results from the 2021 Global Burden of Disease Study. BMC Public Health. 2024;24:2426.

[5] Le Foll B, Piper ME, Fowler CD, et al. Tobacco and nicotine use. Nat Rev Dis Primers. 2022;8:19.

[6] Cho S, Rehni AK, Dave KR. Tobacco use: a major risk factor of intracerebral hemorrhage. J Stroke. 2021;23:37–50.

[7] Jolink WMT, Wiegertjes K, Rinkel GJE, Algra A, de Leeuw FE, Klijn CJM. Location-specific risk factors for intracerebral hemorrhage: systematic review and meta-analysis. Neurology. 2020;95:e1807–18.

[8] Peng WJ, Li Q, Tang JH, et al. The risk factors and prognosis of delayed perihematomal edema in patients with spontaneous intracerebral hemorrhage. CNS Neurosci Ther. 2019;25:1189–94.

[9] Liu F, Sun P, Cheng Y, et al. Age-period-cohort analysis of long-term trends in ischemic stroke mortality in China caused by specific risk factors from 1990 to 2019. Neuroepidemiology. 2024;58:182–98.

[10] Yao X, Xu Y, Siwila-Sackman E, Wu B, Selim M. The HEP score: a nomogram-derived hematoma expansion prediction scale. Neurocrit Care. 2015;23:179–87.

[11] Dimitriadis K, Narkiewicz K, Leontsinis I, et al. Acute effects of electronic and tobacco cigarette smoking on sympathetic nerve activity and blood pressure in humans. Int J Environ Res Public Health. 2022;19:3237.

[12] Saaoud F, Shao Y, Cornwell W, Wang H, Rogers TJ, Yang X. Cigarette smoke modulates inflammation and immunity via reactive oxygen species-regulated trained immunity and trained tolerance mechanisms. Antioxid Redox Signal. 2023;38:1041–69.

[13] Gardi C, Valacchi G. Cigarette smoke and ozone effect on murine inflammatory responses. Ann N Y Acad Sci. 2012;1259:104–11.

[14] Heldt NA, Seliga A, Winfield M, et al. Electronic cigarette exposure disrupts blood-brain barrier integrity and promotes neuroinflammation. Brain Behav Immun. 2020;88:363–80.

[15] GBD 2021 Risk Factors Collaborators. Global burden and strength of evidence for 88 risk factors in 204 countries and 811 subnational locations, 1990–2021: a systematic analysis for the global burden of disease study 2021. Lancet. 2024;403:2162–203.

[16] GBD 2021 Causes of Death Collaborators. Global burden of 288 causes of death and life expectancy decomposition in 204 countries and territories and 811 subnational locations, 1990–2021: a systematic analysis for the global burden of disease study 2021. Lancet. 2024;403:2100–32.

[17] GBD 2021 Diseases and Injuries Collaborators. Global incidence, prevalence, years lived with disability (YLDs),

disability-adjusted life-years (DALYs), and healthy life expectancy (HALE) for 371 diseases and injuries in 204 countries and territories and 811 subnational locations, 1990–2021: a systematic analysis for the global burden of disease study 2021. Lancet. 2024;403:2133–61.
[18] Intracerebral hemorrhage—level 4 cause | institute for health metrics and evaluation. Available at: Institute for Health Metrics and Evaluation website. Accessed November 18, 2024.
[19] Tobacco smoke—level 2 risk | institute for health metrics and evaluation. Available at: Institute for Health Metrics and Evaluation website. Accessed November 18, 2024.
[20] Hankey BF, Ries LA, Kosary CL, et al. Partitioning linear trends in age-adjusted rates. Cancer Causes Control. 2000;11:31–5.
[21] Cao F, Xu Z, Li XX, et al. Trends and cross-country inequalities in the global burden of osteoarthritis, 1990–2019: a population-based study. Ageing Res Rev. 2024;99:102382.
[22] Jiang CY, Han K, Yang F, et al. Global, regional, and national prevalence of hearing loss from 1990 to 2019: a trend and health inequality analyses based on the global burden of disease study 2019. Ageing Res Rev. 2023;92:102124.
[23] Handbook on health inequality monitoring with a special focus on low- and middle-income countries. Available at: The World Health Organization website. Accessed November 18, 2024.
[24] Cao F, Li DP, Wu GC, et al. Global, regional and national temporal trends in prevalence for musculoskeletal disorders in women of childbearing age, 1990-2019: an age-period-cohort analysis based on the global burden of disease study 2019. Ann Rheum Dis. 2024;83:121–32.
[25] Fu W. A Practical Guide to Age–Period–Cohort Analysis: The Identification Problem and Beyond. Chapman and Hall/CRC; 2018.
[26] Age period cohort analysis tool. Available at: National Cancer Institute website. Accessed January 16, 2025.
[27] Bai Z, Wang H, Shen C, An J, Yang Z, Mo X. The global, regional, and national patterns of change in the burden of non-malignant upper gastrointestinal diseases from 1990 to 2019 and the forecast for the next decade. Int J Surg. 2025;111(1):80–92.
[28] Huang D, Lai H, Shi X, et al. Global temporal trends and projections of acute hepatitis E incidence among women of childbearing age: age-period-cohort analysis 2021. J Infect. 2024;89:106250.
[29] Knoll M, Furkel J, Debus J, Abdollahi A, Karch A, Stock C. An R package for an integrated evaluation of statistical approaches to cancer incidence projection. BMC Med Res Methodol. 2020;20:257.
[30] R-forge: Projections using bayesian APC model: project home. Available at: R-Forge website. Accessed January 20, 2025.
[31] GitHub where software is built. Available at: github website. Accessed January 20, 2025.
[32] Reitsma MB, Kendrick PJ, Ababneh E, et al. Spatial, temporal, and demographic patterns in prevalence of smoking tobacco use and attributable disease burden in 204 countries and territories, 1990–2019: a systematic analysis from the global burden of disease study 2019. Lancet. 2021;397:2337–60.
[33] Doty MM, Tikkanen RS, FitzGerald M, Fields K, Williams RD. Income-related inequality in affordability and access to primary care in eleven high-income countries. Health Aff (Millwood). 2021;40:113–20.
[34] Yuan L, Cao J, Wang D, Yu D, Liu G, Qian Z. Regional disparities and influencing factors of high quality medical resources distribution in China. Int J Equity Health. 2023;22:8.
[35] Owolabi MO, Thrift AG, Martins S, et al.; Stroke Experts Collaboration Group. The state of stroke services across the globe: report of world stroke organization-world health organization surveys. Int J Stroke. 2021;16:889–901.
[36] Peters SAE, Huxley RR, Woodward M. Smoking as a risk factor for stroke in women compared with men: a systematic review and meta-analysis of 81 cohorts, including 3,980,359 individuals and 42,401 strokes. Stroke. 2013;44:2821–8.
[37] Chen X, Zheng J, Wang J, et al. Global burden and cross-country inequalities in stroke and subtypes attributable to diet from 1990 to 2019. BMC public health. 2024;24:1813.
[38] Huang B, Chen A, Sun Y, He Q. The role of aging in intracerebral hemorrhage. Brain Sciences. 2024;14:613.
[39] West R. Tobacco smoking: health impact, prevalence, correlates and interventions. Psychol Health. 2017;32:1018–36.
[40] Dai X, Gakidou E, Lopez AD. Evolution of the global smoking epidemic over the past half century: strengthening the evidence base for policy action. Tob Control. 2022;31:129–37.
[41] Peruga A, López MJ, Martinez C, Fernández E. Tobacco control policies in the 21st century: achievements and open challenges. Mol Oncol. 2021;15:744–52.
[42] Frazer K, Callinan JE, McHugh J, et al. Legislative smoking bans for reducing harms from secondhand smoke exposure, smoking prevalence and tobacco consumption. Cochrane Database Syst Rev. 2016;2:CD005992.
[43] Magid-Bernstein J, Girard R, Polster S, et al. Cerebral hemorrhage: pathophysiology, treatment, and future directions. Circ Res. 2022;130:1204–29.